Supporting Information for "Application of Vector Spherical Harmonics to the Magnetisation of Mars' Crust"

David Gubbins[1,2], Yi Jiang[2], Simon E. Williams[3], Keke Zhang[2]

[1]School of Earth and Environment, University of Leeds, UK

[2]State Key Laboratory of Lunar and Planetary Science, Macau University of Science and Technology, Macau

[3]State Key Laboratory of Continental Dynamics, Department of Geology, Northwest University, Xi'an, China

Figures S1–S3 give the VSH decomposition of the radial component of VIM. S1 is the $\mathcal{E}$ part, which reflects the magnetising dipole. These structures are invisible: they produce no external potential field but do produce a potential field internal to the shell that would contribute to the magnetisation of deeper shells. Its contribution would be much weaker than that of the dynamo-generated field and can be ignored, but after dynamo action ceased it would provide secondary magnetisation of the deeper layers.

S2 shows the $\mathcal{I}$ part. It is quite different from the $\mathcal{E}$ part and is mainly concentrated about the equator. This is the part that produces an external potential field that can be observed. Note the labelling on the colour bars, it is almost an order of magnitude smaller than the corresponding $\mathcal{E}$ part.

S3 shows the $\mathcal{T}$ part, which has no radial component.

S4 is the sum of $\mathcal{E}$ and $\mathcal{T}$ parts. This is the entire invisible part of the VIM. In a damped inversion of VIM from magnetic data this would represent the annihilator or null space.

S5 is for the magnetic field. The important point to note is its concentration on the equator for all orientations of the magnetising dipole. It shows that demagnetising the Northern Hemisphere, or in this case removing the magnetic layer, does not produce the observed dichotomy in magnetic field, instead it produces an equatorial ring.

S6 follows the format of Figure 5 in the paper for the Hellas basin, but for the Isidis crater. The crustal thickness model produces an anomaly that is weaker than the one at Hellas because the surrounding crust is thinner there and the crater edges do not seem to be as steep, but the anomaly is not removed by minimum curvature interpolation. The rings are an artefact of the interpolation.

S7 is for the Argyre crater and the same comments apply as to the other 2.

S8 shows the Lowes spectra for the observed field and the original crustal thickness model. The crustal thickness grid has more energy at short and long wavelengths but the spectra are broadly similar, indicating the anomalies observed at satellite altitude could arise from variations in crustal thickness.

Table ST1 gives RMS amplitudes

	Original	A	B
$\mathcal{E}$ kA	1970	1950 (-1.02%)	2040 (-3.55%)
$\mathcal{I}$ kA	231	235 (+1.73%)	166 (-28.14%)
$\mathcal{T}$ kA	218	221 (+1.38%)	199 (-8.26%)
$\mathcal{E} : \mathcal{I} : \mathcal{T}$	81:10:9	81:10:9	85:7:8

Table S1. RMS of $\mathcal{EIT}$ components derived by the crustal thicknesses shown in Figure 5. Original: From inversion of topography and gravity data shown in Figure 2; A: layer thickness within the crater region replace with minimum curvature interpolation, (c) in Figure 5; B: crater filled in, (d) in Figure 5). The percentage of change has been shown in the Brackets.

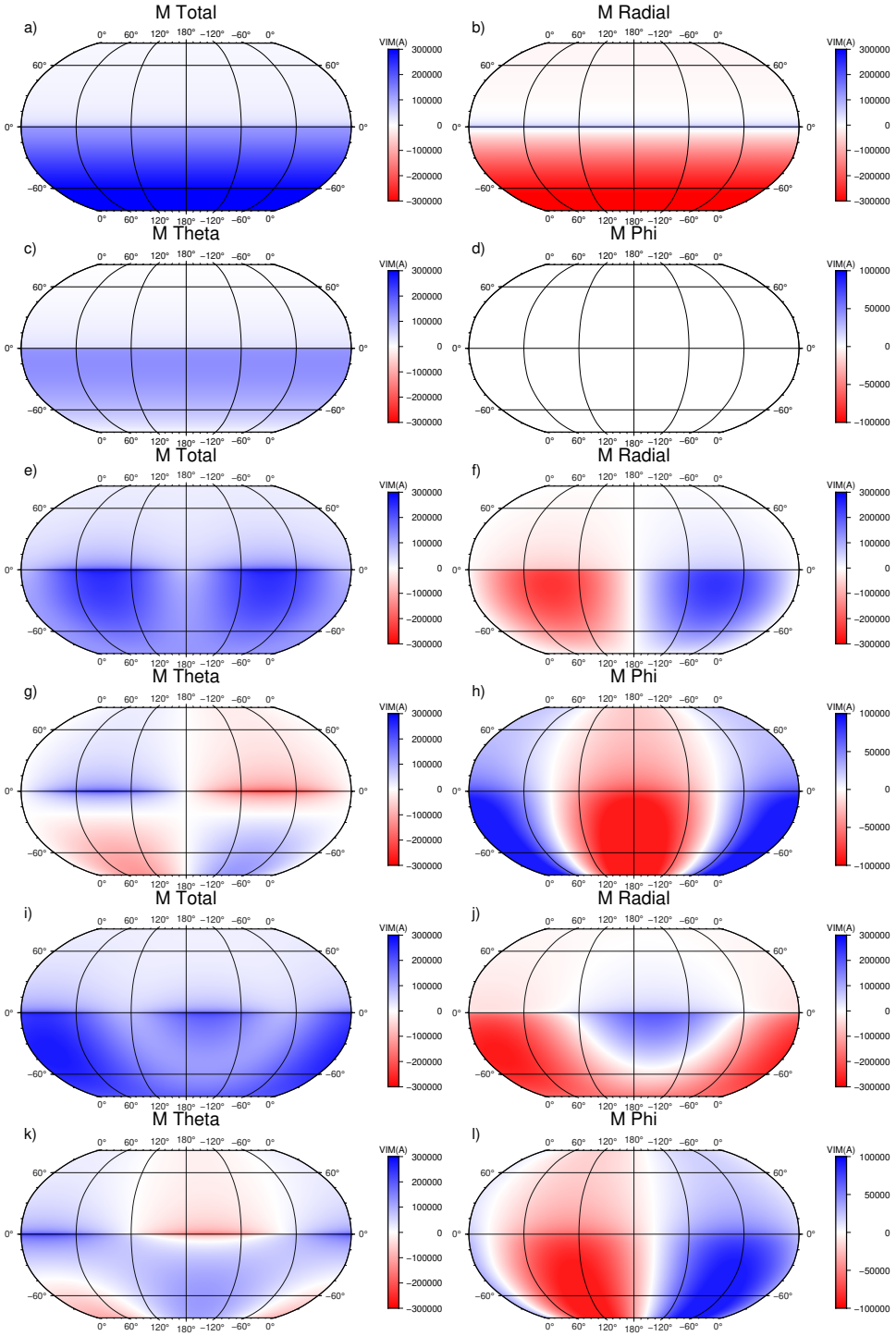

Figure S1. The $\mathcal{E}$ part of the VIM for different magnetising dipoles and a crust with thickness 0 in the Northern Hemisphere and 40 km in the Southern Hemisphere. a-d is for an internal axial dipole, a: M, b: M_r, c: M_θ, d: M_ϕ; e-h is for an equatorial dipole, pole at 0°N,270°E, e: M, f: M_r, g: M_θ, h: M_ϕ; i-l is for a dipole with paleopole 34°N,202°E, i: M, j: M_r, k: M_θ, l: M_ϕ.

[width=30pc]I(si).pdf

Figure S2. As Figure S1 for the $\mathcal{I}$ part.

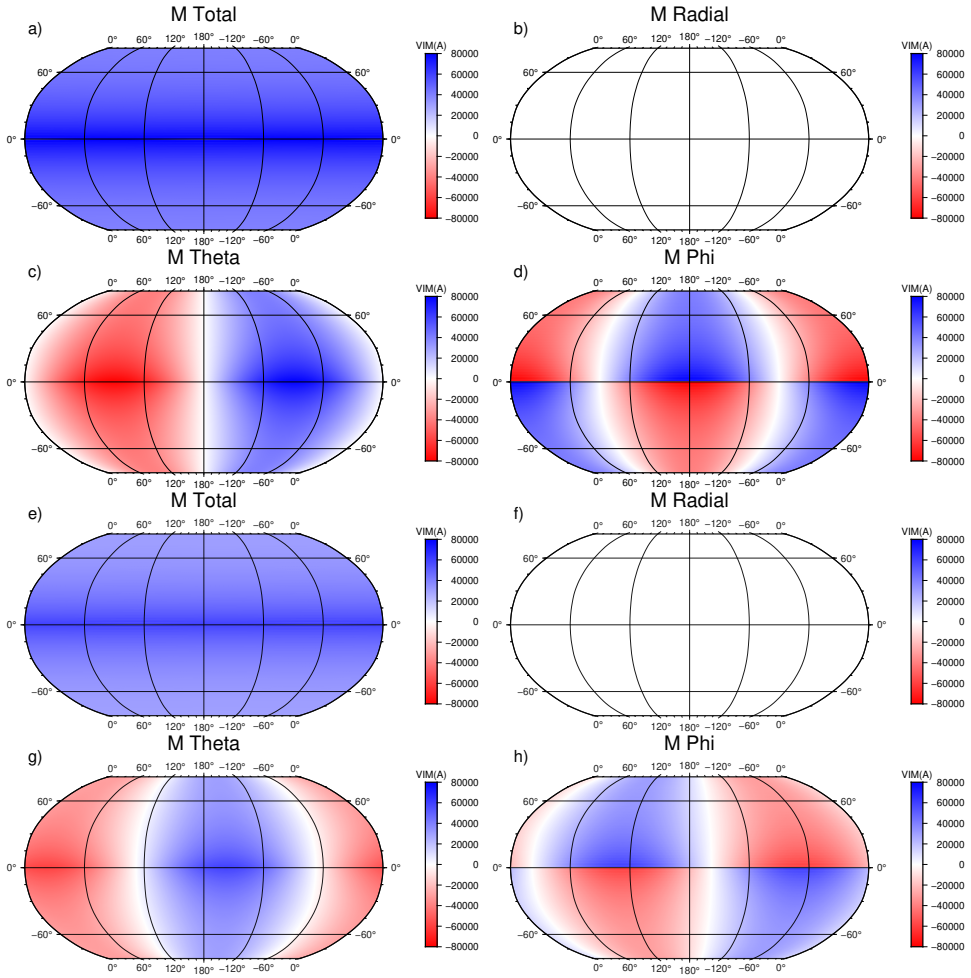

Figure S3. As Figure S1(e-l) for the $\mathcal{T}$ part. $\mathcal{T}$ part for axial dipole are zero and therefore not shown.

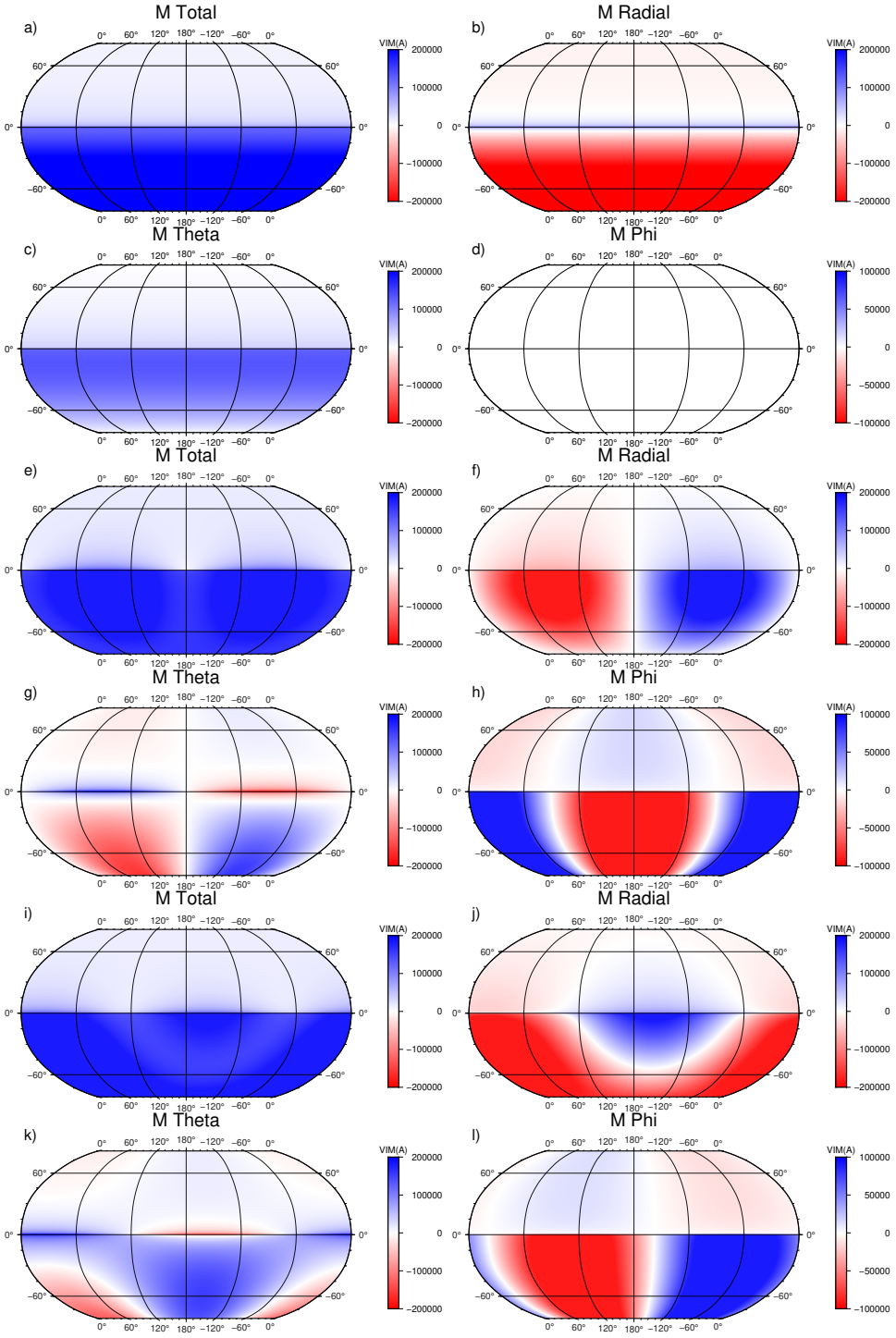

Figure S4. As Figure S1 for the sum $\mathcal{E} + \mathcal{T}$. This combination is the entire "invisible" part of the VIM.

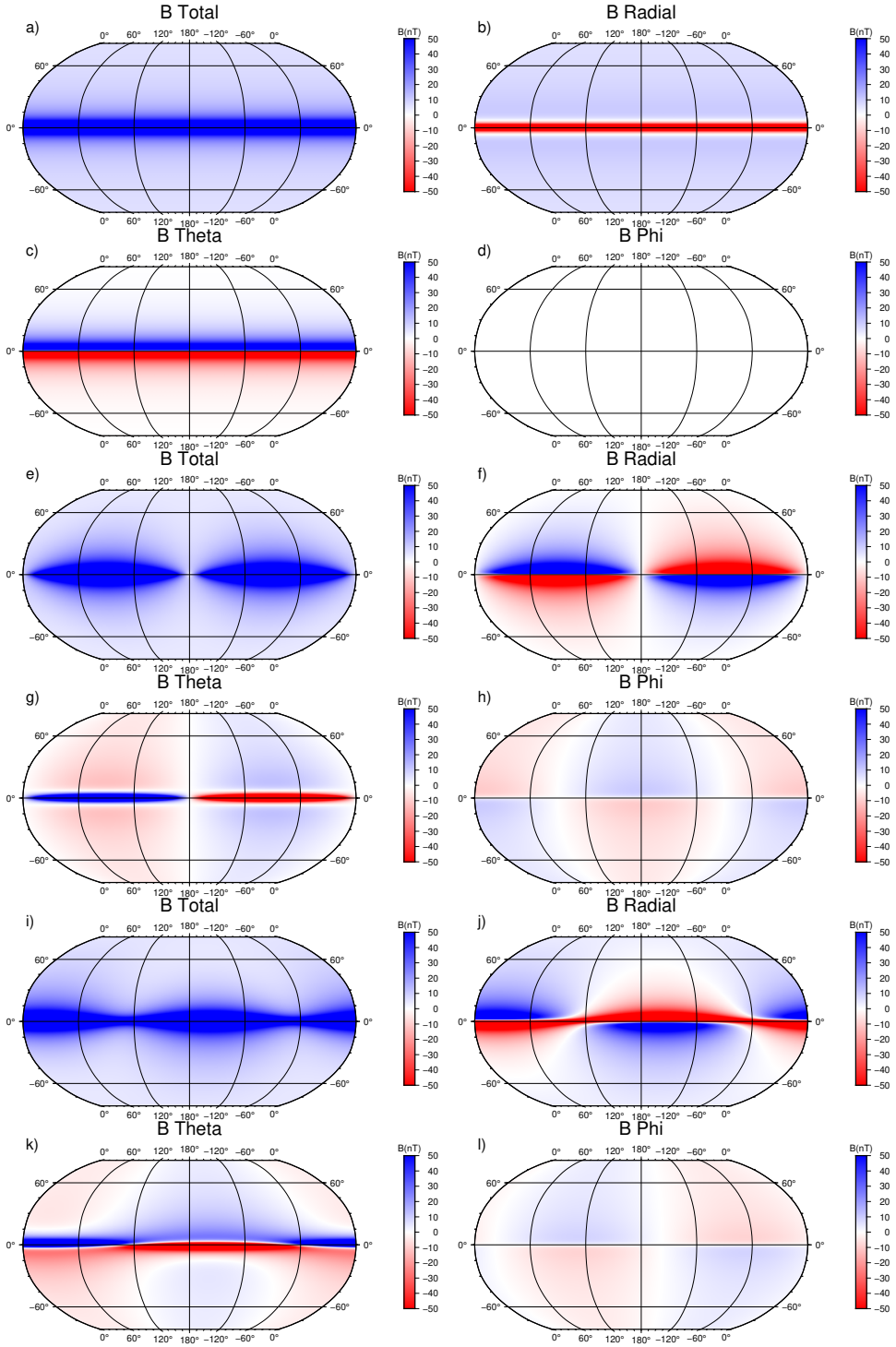

Figure S5. As Figure S1 for the magnetic field.

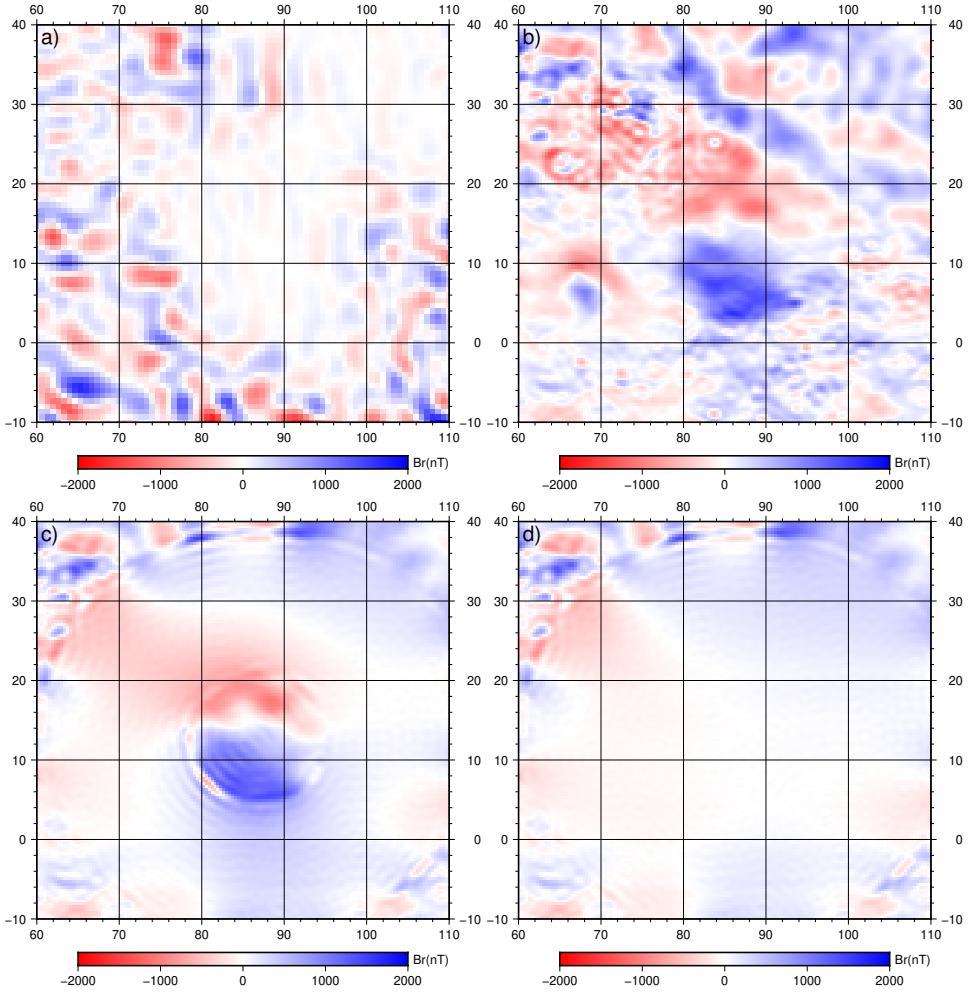

Figure S6. Close-up of the Isidis anomaly illustrating radial component of the magnetic field. a: the satellite model; b: original crustal thickness model; c: model with smoothed crater edges; d: crater filled in.

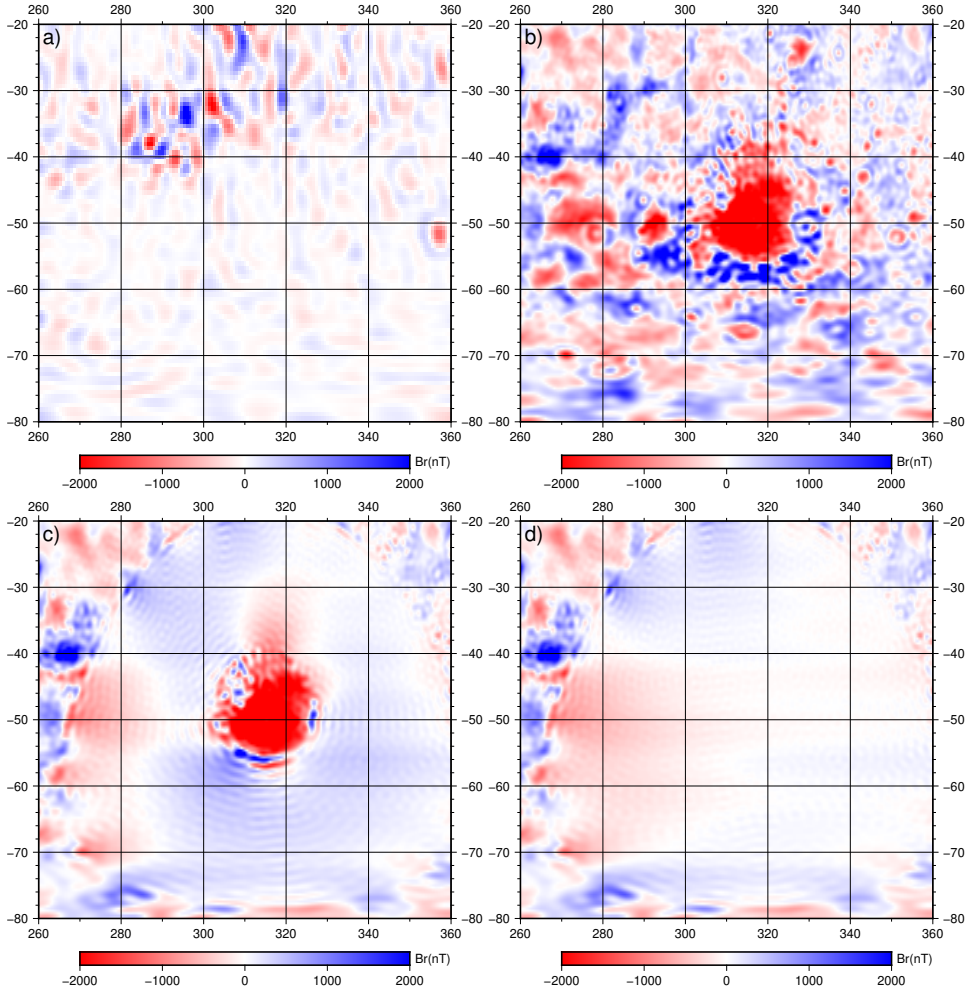

Figure S7. As Figure S6 for the Argyre anomaly.

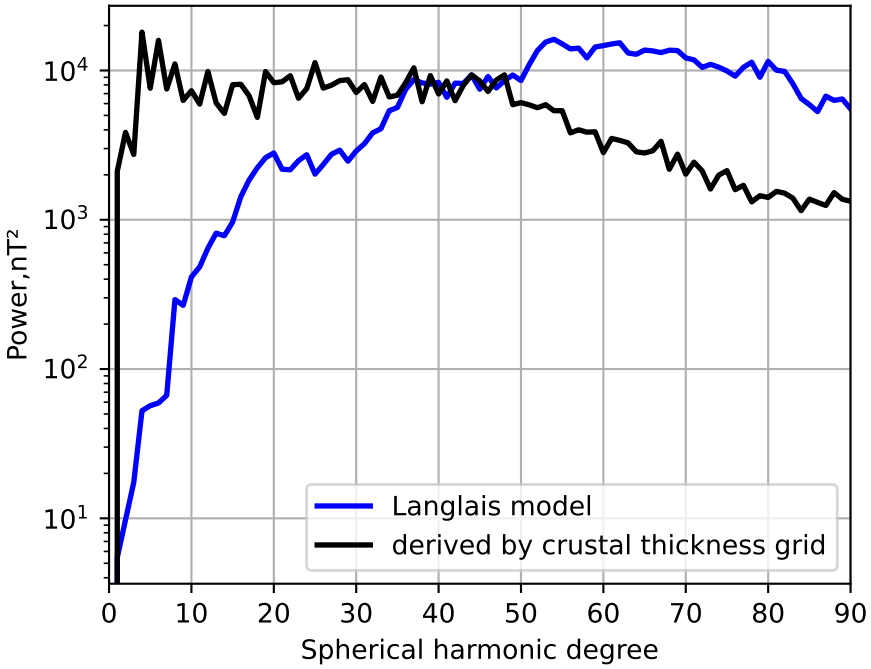

Figure S8. Lowes spectra of the satellite model(blue) and original crustal thickness model(black).